

Stimulated Emission Pumping Spectroscopy of the $[\tilde{X}]^1A'$ State of CHFCalvin Mukarakate,[†] Chong Tao,[†] Christopher D. Jordan,[‡] William F. Polik,^{*,‡} and Scott A. Reid^{*,†}

Department of Chemistry, Marquette University, Milwaukee, Wisconsin 53201-1881, and Department of Chemistry, Hope College, Holland, Michigan 49422-9000

Received: September 4, 2007; In Final Form: October 24, 2007

We have recorded stimulated emission pumping (SEP) spectra of the $\tilde{A}^1A'' \rightarrow \tilde{X}^1A'$ system of CHF, which reveal rich detail concerning the rovibronic structure of the \tilde{X}^1A' state up to $\sim 7000 \text{ cm}^{-1}$ above the vibrationless level. Using several intermediate \tilde{A}^1A'' state levels, we obtained rotationally resolved spectra for 16 of the 33 levels observed in our previous single vibronic level (SVL) emission study (Fan et al., *J. Chem. Phys.* **2005**, *123*, 014314), in addition to one new level. An anharmonic effective Hamiltonian model poorly reproduces the term energies even with the improved set of data because of the extensive interactions among levels in a given polyad (p) having combinations of ν_1 , ν_2 , ν_3 , which satisfy the relationship $p = 2\nu_1 + \nu_2 + \nu_3$. However, the precise A rotational constants determined from the SEP data were invaluable in clarifying the assignments for these strongly perturbed levels, and the data are well reproduced using a multiresonance effective Hamiltonian model. The derived vibrational parameters are in good agreement with high level *ab initio* calculations. The experimental frequencies were combined with those of CDF to derive a harmonic force field and average (r_z , r_o^z) structures for the ground state.

Introduction

Carbenes are important reactive intermediates that are found in organic synthesis, combustion, thermal decomposition of small organic molecules, and atmospheric and interstellar chemistry.^{1–13} The chemistry of carbenes is fascinating because the divalent carbon gives rise to low-lying singlet and triplet states with similar energies but distinct chemical reactivity. A central issue in carbene chemistry, and the focus of many theoretical and some experimental studies over the years, has been the precise determination of the singlet–triplet energy gap, ΔE_{TS} .^{14–40}

The monohalocarbene CHF is the smallest carbene with a singlet ground state, and is thus a prototype for exploring the spectroscopy, dynamics, Renner–Teller effect in and electronic structure of singlet carbenes.^{14–34,41–59} Using laser spectroscopy, recent progress has been made on the experimental side in probing the vibrational structure of the \tilde{X}^1A' state and spin–orbit coupling for the set of monohalocarbenes HCX (X = F, Cl, and Br).^{34,36–40,60–65} For example, SVL emission spectra of CHCl, CDCl, CHBr, and CDBr show transitions to triplet levels, which borrow intensity from nearby levels of the \tilde{X}^1A' state.^{36–40,60–65} Experimental estimates for the magnitude of ΔE_{TS} derived from the emission studies are in very good agreement with theoretical predictions.^{36–40,61–65}

We previously reported single vibronic level (SVL) emission spectra of CHF and CDF which mapped the vibrational levels up to $\sim 10,000 \text{ cm}^{-1}$ above the vibrationless level of the \tilde{X}^1A' state, encompassing the region where the triplet origin is predicted. (Theoretical values for ΔE_{ST} range from 4617 to 5537 cm^{-1} ,^{14–22,24–27,29–33} while an experimental value of $5210 \pm$

140 cm^{-1} was derived from photoelectron spectra of CHF²⁸.) An anharmonic effective Hamiltonian model well reproduced the experimental term energies of CDF. However, the spectra of CHF were complicated by Fermi resonances among levels in a given polyad (p) having combinations of ν_1 , ν_2 , and ν_3 , which satisfied the relationship $p = 2\nu_1 + \nu_2 + \nu_3$.⁶⁰ Because of the extensive anharmonic interactions, the assignments for many levels of CHF were considered tentative.

In this study, we have applied rotationally resolved stimulated emission pumping (SEP) spectroscopy to probe the vibrational mixing in the \tilde{X}^1A' state and identify spin–orbit interactions with the low lying \tilde{a}^3A'' state, which have previously been observed in the \tilde{A}^1A'' state using quantum beat spectroscopy.⁵⁶ Suzuki and Hirota reported emission and high-resolution SEP spectroscopy from the 0^0 level of CHF,⁵⁰ identifying a resonance between 1_1 and 2_13_1 and an unusually small anharmonic C–H stretching frequency [$2643.0393(26) \text{ cm}^{-1}$]. However, their study investigated only a few levels up to 3000 cm^{-1} above the vibrationless level of the \tilde{X}^1A' state. Building upon this work and our previous studies using fluorescence excitation⁵⁶ and SVL emission⁶⁰ spectroscopy, we have extended the SEP studies up to $\sim 7000 \text{ cm}^{-1}$ above the vibrationless level of the \tilde{X}^1A' state. The precise A rotational constants determined from the SEP data have clarified the assignments for many levels, and we have modeled the data using a two-resonance effective Hamiltonian model. The derived vibrational parameters are in excellent agreement with high level *ab initio* calculations, and the experimental harmonic frequencies are combined with those of CDF to derive a harmonic force field and average (r_z) structure for the ground state.

Experimental Procedures

The apparatus, pulsed discharge nozzle, and data acquisition procedures have been described in previous studies.^{55–66} CHF was generated by a pulsed electrical discharge through a 1% to

* Corresponding author. E-mail: scott.reid@mu.edu (S.A.R.); polik@hope.edu (W.F.P.).

[†] Marquette University.

[‡] Hope College.

2% mixture of CH₂F₂ (Aldrich, 99.9%) in argon (BOC gases, 99.999%) that was premixed in a 1 L stainless steel cylinder. The mixture was continuously expanded through a pulsed nozzle at backing pressures of ~ 2 bar. The discharge was initiated by a +1 kV pulse of ~ 100 μ s duration, through a current-limiting 100 k Ω ballast resistor.

The timing of the lasers, nozzle, and discharge pulse firing was controlled by two digital delay generators (Stanford Research Systems DG535), one of which generated a variable width gate pulse for the high voltage pulser (Directed Energy GRX-1.5K-E). The pump laser beam (was generated from a tunable dye laser (Spectra Physics PDL-3, line width ~ 0.3 cm⁻¹) pumped by the second harmonic of a Nd:YAG laser (Powerlite 7010); this beam excited specific rovibrational transitions in the $\tilde{A} \leftarrow \tilde{X}$ system. After a delay of approximately 400–500 ns, a counter propagating beam from a second dye laser (Lambda-Physik Scanmate 2E, line width ~ 0.15 cm⁻¹), pumped by the second or third harmonic of a Nd:YAG laser (Continuum NY-61), stimulated emission to the \tilde{X} state or excited transitions in the $\tilde{B} \leftarrow \tilde{A}$ system.⁶⁶ The laser beams were not focused, and typical pulse energies were ~ 1 –2 mJ for the pump and ~ 10 mJ for the dump in an ~ 3 mm diameter beam.

A mutually orthogonal geometry of lasers, molecular beam, and detector was used, where the two overlapped lasers crossed the molecular beam at ~ 1 cm downstream. Fluorescence was collected and collimated by a 2 in. diameter, $f/2.4$ plano-convex lens and filtered via an appropriate cutoff filter (Corion or Edmund Scientific) prior to striking a photomultiplier tube detector (PMT; Oriol 77348) held at -700 V. Typically, long-pass filters with cut-on wavelengths longer than the dump wavelength were used; however, in experiments where the 1_0^1 2_0^1 level was pumped, a short-pass filter with a cutoff wavelength of 600 nm was used. The signal from the PMT was fed to dual boxcar integrators (Stanford Research Systems SR250), and the SEP signal was obtained by integrating a portion of the fluorescence decay before and after the dump laser pulse. The ratio of signal from each gate was recorded to remove the effect of shot-to-shot fluctuations in the signal. Typically, 10 shots were averaged at each wavelength step of 0.002 nm.

The wavelength of the first laser was calibrated using the well-known $\tilde{A} \leftarrow \tilde{X}$ spectroscopic constants.⁵⁶ The second laser was calibrated using optogalvanic transitions in Ar or Ne; we estimate an absolute calibration error of less than 0.5 cm⁻¹. The SEP lines were fit to a Gaussian line shape function, using Origin 7.5 software, and the transition frequencies were least-squares fit to an asymmetric top Hamiltonian to derive the vibrational term energy and rotational constants, using the upper state constants determined in our previous work.⁵⁶

Results and Discussion

We obtained SEP spectra from four intermediate $\tilde{A}1A''$ state levels, 0_0^0 , 2_0^2 , $2_0^1 3_0^1$, and $1_0^2 1_0^1$, being careful to select levels that were not perturbed by Renner–Teller or spin–orbit interactions.⁵⁶ Figure 1 displays typical spectra, which feature fluorescence depletions of 10–20%. Note that the broader peaks in Figure 1 reflect upward transitions to the \tilde{B} state, as we recently reported.⁶⁶ The pump and dump transitions follow C-type selection rules ($\Delta J = 0, \pm 1$; $\Delta K_a = \pm 1$; $\Delta K_c = 0, \pm 2$). Consequently, a maximum of five lines are observed when pumping transitions with $K_a' = 1$ in the \tilde{A} state, as shown in Figure 1. The ~ 20 K rotational temperature of our beam limited the pump transitions to excited-state levels with $K_a' = 0, 1$, and 2.

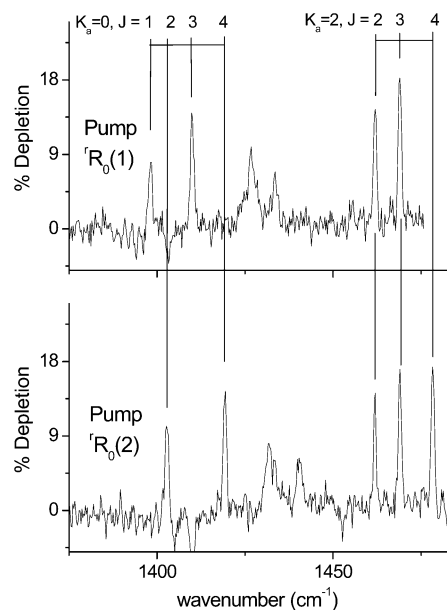


Figure 1. SEP spectra (inverted for clarity) for CHF $\tilde{X}(0,1,0)$. These correspond to pumping $K_a' = 1$ in the \tilde{A} state; the upper panel displays the spectrum obtained by pumping rotational line $J = 2$ and the lower panel is for pumping $J = 3$. The spectra reflect a 10 shot average, and the x-axis labels the shifts in frequency from the excitation line.

TABLE 1: Vibrational Term Energies and Rotational Constants (in cm⁻¹) for CHF Derived from SEP Spectroscopy

assignment ^a	A ^b	\bar{B} ^c	band origin ^d
(0,1,0)	15.96	1.180	1403.2
(0,0,2)	15.46	1.145	2364.3
(0,1,1)	15.74	1.165	2568.3
(1,0,0)	15.32	1.194	2642.9
(0,2,0)	16.20	1.171	2812.7
(0,1,2)	15.74	1.149	3729.4
(1,0,1)	15.21	1.158	3835.7
(1,1,0)	15.73	1.171	3936.5
(0,2,1)	15.91	1.162	4017.4
(0,3,0)	16.48	1.167	4220.7
(1,0,2) ^e	15.27	1.148	5008.5
(0,2,2)	15.23	1.153	5075.6
(2,0,0)	15.11	1.174	5134.7
(1,2,0)	16.06	1.197	5295.6
(0,4,0)	16.81	1.165	5617.3
(2,1,0)	15.36	1.199	6372.0
(1,3,0)	16.32	1.161	6640.1
(0,5,0)	17.16	1.166	7001.7

^a Approximate assignment based on the two-resonance effective Hamiltonian model (Model 3; see text). ^b Estimated uncertainty of ± 0.04 cm⁻¹. ^c Estimated uncertainty of ± 0.010 cm⁻¹. ^d Estimated uncertainty of ± 0.5 cm⁻¹. ^e Not observed in previous emission studies.

Table 1 presents the fit parameters for the measured bands, which are in good agreement with previous data for high-resolution SVL emission⁴⁹ and SEP spectroscopy.⁵⁰ We measured SEP spectra for 17 levels, including one level that was not observed in our SVL emission study.⁶⁰ For each level, the A and $\bar{B} = (B + C)/2$ rotational constants were determined. Because the A constant is very sensitive to the quanta of bending excitation, as shown in Figure 2, it is helpful in clarifying the vibrational assignments. Initially, we performed a fit of the observed A constants to following the expression:

$$A_{v_1, v_2, v_3} = A_0 + \sum_i \alpha_i v_i \quad (1)$$

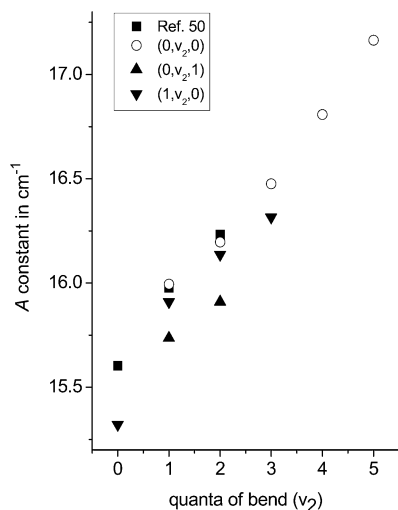


Figure 2. Dependence of the A rotational constant on the bending quantum number for the pure bending and combination states in CHF (\bar{X}^1A'), derived from the SEP data. For comparison, previous results from Hirota and co-workers⁵⁰ are shown.

which returned the parameters (in cm^{-1}): $\alpha_1 = -0.26(9)$, $\alpha_2 = 0.27(5)$, $\alpha_3 = -0.21(7)$, and $A_0 = 15.69(15)$. The standard deviation of this fit (0.20 cm^{-1}) was far in excess of our experimental uncertainty ($\sim 0.04 \text{ cm}^{-1}$), reflecting the fact that any vibrational assignment of the levels in CHF is only approximate, as anharmonic mixing destroys the traditional normal mode labels.

The SEP and SVL emission data were combined in a nonlinear least-squares fit to several different effective Hamiltonian models. Model 1 was the standard anharmonic model (Dunham expansion) referenced to the vibrationless level:⁶⁷

$$G^0(v_1, v_2, v_3) = \sum_{i=1}^3 v_i \omega_i^0 + \sum_{j \geq i, i=1}^3 v_i v_j x_{ij}^0 \quad (2)$$

where ω_i^0 is the harmonic frequency of mode i , x_{ij}^0 is a diagonal anharmonicity constant, and x_{ij}^0 is an off-diagonal or cross-anharmonicity constant. Resonance-effective Hamiltonian models (Models 2 and 3) were employed, which included one (k_{123}) and two (k_{122} and k_{123}) Fermi resonance matrix elements, respectively, of the form

$$\langle v_1, v_2, v_3 | H_F | v_1 - 1, v_2 + 1, v_3 + 1 \rangle = k_{123} [(v_1)(v_2 + 1)(v_3 + 1)/8]^{0.5} \quad (3)$$

and

$$\langle v_1, v_2, v_3 | H_F | v_1 - 1, v_2 + 2, v_3 \rangle = k_{122} [(v_1)(v_2 + 1)(v_2 + 2)/8]^{0.5} \quad (4)$$

The fit parameters and standard deviations for all three models are given in Table 2, along with the results of *ab initio* calculations from a quartic potential energy surface computed at the CCSD(T)/aug-cc-pVQZ level. The MOLPRO program⁶⁸ was used to optimize the geometry of CHF and compute energies of displaced geometries, which allowed the determination of the quadratic, cubic, and quartic force constants by numerical differences. A modified version of the SPECTRO program⁶⁹ was then used to calculate the harmonic frequencies, anharmonic constants, and resonance constants from the computed equilibrium geometry and force field. The anharmonic constants were calculated using second-order perturbation

theory,⁷⁰ from which the resonances were removed and treated explicitly.^{71,72} Note the good agreement between experiment and *ab initio* constants for each model, and the marked improvement in the fit for the one- and two-resonance models. The latter reproduces the term energies to within 2 cm^{-1} , which is similar to the fit standard deviation obtained in our SVL emission study of CDF.⁶⁰ Lists of assignments and fit deviations for each model are provided in Table 3.

A consequence of the strong Fermi resonance interactions in CHF, evidenced in the large third-order constants k_{122} and k_{123} (Table 2), is extensive mixing of the levels within a given polyad. This is readily shown in the mixing coefficients, which describe the zeroth-order composition of the eigenstates, which were determined from our analysis. For example, in the polyad with $p = 4$, which contains seven levels and extends over 600 cm^{-1} , the purest state is the highest lying member at 5617.3 cm^{-1} , which comprises $\sim 70\%$ 2^4 and $\sim 27\%$ 1^{12} , with smaller contributions from other zeroth-order states. This finding that the bending overtone in a given polyad most closely resembles the pure normal mode state is quite general and explains the good linear correlation shown in Figure 2. A detailed listing of the wavefunctions produced from the POLYAD program⁷³ is provided in the Supporting Information.

Converting the fit frequencies to harmonic frequencies using the relationship:⁶⁷

$$\omega_i = \omega_i^0 - x_{ii}^0 - \sum_{j \neq i} x_{ij}^0/2 \quad (5)$$

(note the typographical error in this formula given in our previous report⁶⁰), we obtain (in cm^{-1}) $\omega_1 = 2785.2(48)$, $\omega_2 = 1445.1(16)$, and $\omega_3 = 1211.2(27)$. In comparison, high level *ab initio* calculations give values (in cm^{-1}) ranging from 2767 to 2815 for ω_1 , 1433–1448 for ω_2 , and 1171–1206 for ω_3 .^{33,54,60} We used the derived harmonic frequencies and reported centrifugal distortion constants of CHF^{50,74} and CDF⁴⁶ to perform a normal-mode analysis, with the harmonic force field refined using the ASYM40 program of Hedberg and Mills.⁷⁵ Table 4 presents the fit results and harmonic force constants. We were able to derive the entire force constant matrix save one off-diagonal element, f_{12} , which was set to zero in the fit.

The harmonic corrections to the CHF and CDF rotational constants determined from the force field were used in a least-squares analysis to compute an average (r_z) structure for CHF. In our analysis, allowance was made for a 0.0035 \AA Laurie contraction of the C–H bond upon deuteration, calculated using the following expression:^{76,77}

$$\delta r_z = 3/2 a \delta \langle u^2 \rangle - \delta K \quad (6)$$

where the difference in mean square displacement, $\langle u^2 \rangle$, and perpendicular amplitude correction δK were obtained from the force field, and the Morse anharmonicity parameter (a ; units of \AA^{-1}) was estimated from data for the corresponding diatomic (C–X) molecules⁷⁸ input into the following expression:⁷⁹

$$a = 2/3 \pi \omega_e \sqrt{\frac{c\mu}{2h(B_e)^3}} \left(\alpha_e + \frac{6(B_e)^2}{\omega_e} \right) \quad (7)$$

An r_e^z structure was also determined using the following relationship:⁸⁰

$$r_e^z = r_z - 3/2 a \langle u^2 \rangle + K \quad (8)$$

TABLE 2: Comparison of the Derived Vibrational Parameters (in cm^{-1}) for the \tilde{X} State of CHF for the Three Effective Hamiltonian Models Described in the Text^a

parameter	Model 1		Model 2		Model 3	
	exp.	calc.	exp.	calc.	exp.	calc.
ω_1^0	2727(31)	2670.6	2684.2(81)	2662.4	2706.0(39)	2697.3
ω_2^0	1414(7)	1385.2	1414.9(16)	1385.2	1413.7(9)	1402.7
ω_3^0	1196(15)	1196.6	1195.1(63)	1196.6	1200.1(21)	1196.6
x_{11}^0	-81(17)	-71.1	-62.1(40)	-71.1	-62.6(22)	-71.1
x_{12}^0	-82(7)	-118.8	-56.7(13)	-127.0	-37.9(25)	-57.0
x_{13}^0	11(13)	10.1	-0.5(52)	1.9	4.7(24)	1.9
x_{22}^0	-2.9(12)	17.1	-3.0(3)	17.1	-7.8(6)	-0.4
x_{23}^0	-0.4(27)	-17.3	-7.7(9)	-9.0	-9.2(5)	-9.0
x_{33}^0	-13(5)	-9.9	-7.2(33)	-9.9	-8.9(11)	-9.9
k_{122}					-113.4(36)	-103.3
k_{123}			83.5(32)	99.2	95.0(17)	99.2
σ	25.7		5.5		2.1	

^a Also shown are the parameters calculated at the CCSD(T)/aug-cc-pVQZ level.

TABLE 3: Comparison of Assignments and Fit Deviations (in cm^{-1}) for \tilde{X} State Levels of CHF for the Three Effective Hamiltonian Models Described in the Text^a

term energy	Model 1		Model 2		Model 3	
	assignment	O.-C. ^b	assignment	O.-C.	assignment	O.-C.
0	(0,0,0)	0	(0,0,0)	0	(0,0,0)	0
1192	(0,0,1)	-9	(0,0,1)	-4	(0,0,1)	0
1403.2	(0,1,0)	8.3	(0,1,0)	8.7	(0,1,0)	2.7
2364.3	(0,0,2)	-26.1	(0,0,2)	-3.0	(0,0,2)	0.3
2568.3	(0,1,1)	25.2	(0,1,1)	5.6	(0,1,1)	0.8
2642.9	(1,0,0)	3.2	(1,0,0)	-2.7	(1,0,0)	0.0
2812.7	(0,2,0)	4.5	(0,2,0)	5.0	(0,2,0)	2.7
3729.4	(0,1,2)	19.5	(0,1,2)	5.1	(0,1,2)	-0.7
3835.7	(1,0,1)	4.0	(1,0,1)	-3.0	(1,0,1)	2.1
3936.5	(1,1,0)	38.9	(1,1,0)	5.0	(1,1,0)	0.9
4017.4	(0,2,1)	-18.6	(0,2,1)	8.6	(0,2,1)	1.8
4220.7	(0,3,0)	-3.6	(0,3,0)	-3.2	(0,3,0)	-1.5
5008.5	(1,0,2)	-1.9	(1,0,2)	0.1	(1,0,2)	0.4
5075.6	(0,2,2)	78.1	(1,1,1)	-2.4	(0,2,2)	-1.1
5134.7	(2,0,0)	-4.8	(0,2,2)	-4.3	(2,0,0)	2.2
5220	(1,1,1)	-51	(2,0,0)	2	(1,1,1)	-4
5295.6	(1,2,0)	3.2	(1,2,0)	0.5	(1,2,0)	-3.3
5411	(0,3,1)	-12	(0,3,1)	2	(0,3,1)	0
5617.3	(0,4,0)	-6.1	(0,4,0)	-5.9	(0,4,0)	-1.5
6299	(0,2,3)	-17	(0,2,3)	2	(0,2,3)	-2
6372.0	(2,1,0)	4.8	(2,1,0)	6.1	(2,1,0)	1.8
6477	(1,2,1)	15	(1,2,1)	-3	(1,2,1)	1
6640.1	(1,3,0)	-23.7	(1,3,0)	2.0	(1,3,0)	1.3
6798	(0,4,1)	-6	(0,4,1)	-2	(0,4,1)	-1
7001.7	(0,5,0)	-2.3	(0,5,0)	-2.6	(0,5,0)	2.0
7679	(0,3,3)	1.0	(2,2,0)	-8	(2,1,1)	-2
7820	(1,3,1)	-11	(1,3,1)	-6	(1,3,1)	1
7987	(0,4,2)	-41	(1,4,0)	-6	(1,4,0)	-2
8177	(0,5,1)	3	(0,5,1)	-3	(0,5,1)	-1
8384	(0,6,0)	-2	(0,6,0)	-3	(0,6,0)	-2
8951	(1,3,2)	24	(2,3,0)	8	(1,4,1)	1
9336	(0,5,2)	-3	(0,5,2)	3	(0,5,2)	2
9548	(0,6,1)	13	(0,6,1)	-1	(0,6,1)	-1
9749	(0,7,0)	10	(0,7,0)	8	(0,7,0)	2

^a This table includes data from both SEP (this work) and SVL emission⁶⁰ spectroscopy. ^b O.-C., observed-calculated in cm^{-1} .

The derived structural parameters are $r_z(\text{C-H}) = 1.118(1) \text{ \AA}$, $r_z(\text{C-F}) = 1.311(1) \text{ \AA}$, $r_e^z(\text{C-H}) = 1.104(1) \text{ \AA}$, $r_e^z(\text{C-F}) = 1.304(1) \text{ \AA}$, and $\theta_{\text{HCF}} = 103.1(1)^\circ$. In comparison, *ab initio* predictions give equilibrium structural parameters values ranging from 1.120 to 1.126 \AA for $r(\text{C-H})$, 1.309 to 1.324 \AA for $r(\text{C-F})$, and 101.9 to 102.4 $^\circ$ for θ_{HCF} .^{33,54,60} In principle, the vibration-rotation constants (α'_s) determined from a fit of the SEP data could be used to determine an r_e structure; however, this was not attempted because of the poor quality of the fit. In

TABLE 4: Results of the Force Field Analysis of CHF^a

parameter	fitted data			
	CHF observed	CHF O.-C. ^a	CDF observed	CDF O.-C.
ω_1/cm^{-1}	2785.2	-1.7	2049.9	1.7
ω_2/cm^{-1}	1445.1	0.7	1214.3	0.6
ω_3/cm^{-1}	1211.2	0.6	1080.7	1.6
Δ_J/MHz	0.1181	-0.010	0.1004	0.0010
Δ_{JK}/MHz	2.370	0.103	1.478	0.025
Δ_K/MHz	70.99	1.30	25.58	1.89
δ_{JK}/MHz	0.009859	0.000512	0.01245	0.00065
δ_K/MHz	1.684	0.266	1.200	0.190
		force constants		
$f_{11}(\text{mdyn/\AA})$	4.255(10)		$f_{12}(\text{mdyn/\AA})$	0.0(fixed)
$f_{22}(\text{mdyn/\AA})$	1.345(10)		$f_{13}(\text{mdyn/\AA})$	0.455(23)
$f_{33}(\text{mdyn/\AA})$	6.718(10)		$f_{23}(\text{mdyn/\AA})$	0.644(23)
		coordinate notation		
1		C-H stretch		
2		H-C-F bend		
3		C-F stretch		

^a The centrifugal distortion constants were obtained from refs 47, 50, and 68. ^b O.-C., observed-calculated.

an effort to improve the fit, we refit the A constants using eq 1 with effective quantum numbers based upon the wavefunction composition predicted by the POLYAD program. The fit standard deviation decreased by a factor of 2, yet was still twice our experimental uncertainty. In this regard, SEP spectra of the deuterated isotopomer CDF should be useful in obtaining a precise set of rotation-vibration constants for further structural refinement and modeling of the anharmonic CHF force field.

Conclusions

We have recorded stimulated emission pumping (SEP) spectra of the $\tilde{A}^1A' \rightarrow \tilde{X}^1A'$ system of CHF, which reveal rich detail concerning the rovibronic structure of the \tilde{X}^1A' up to 7000 cm^{-1} above the vibrationless level. Spectra were obtained from several intermediate \tilde{A}^1A'' state levels, 0_0^0 , 2_0^2 , $2_0^1 3_0^1$, and $1_0^1 2_0^1$, and we obtained rotationally resolved spectra for 16 of the 33 levels observed in our previous single vibronic level (SVL) emission study,⁶⁰ in addition to one new level. An anharmonic effective Hamiltonian model poorly reproduces the term energies because of the extensive interactions among levels in a given polyad (p) having combinations of ν_1 , ν_2 , and ν_3 , which satisfy the relationship $p = 2\nu_1 + \nu_2 + \nu_3$. However, the precise A rotational constants determined from the SEP data aided in clarifying the assignments for these strongly perturbed levels,

and the use of a multiresonance effective Hamiltonian model improved the fit standard deviation to near the limits of experimental uncertainty. The derived vibrational parameters are in good agreement with high level *ab initio* calculations; these frequencies were combined with those of CDF to derive a harmonic force field and average (r_2) structure for the ground state.

Despite a strongly perturbed vibrational structure in the ground \tilde{X}^1A' state, we have not obtained in this work any evidence for spin-orbit interactions with the low-lying \tilde{a}^3A'' state. Such perturbations have been observed, however, in SVL emission spectra of the heavier monohalocarbenes, and SEP spectroscopy should prove useful in interrogating the structure of the triplet state and spin-orbit mixing in these systems.

Acknowledgment. S.A.R. gratefully acknowledges support of this research by the National Science Foundation under grants CHE-0717960 and CHE-0353596. W.F.P. and C.D.J. gratefully acknowledge the National Science Foundation (CHE-0520704 and CHE-0624602) and the Howard Hughes Medical Institute for computing resources and stipend support to carry out this research. We thank Dr. Scott H. Kable for experimental assistance and helpful advice regarding this work, and John L. Davisson for assistance with the analysis.

Supporting Information Available: Wave functions for the observed eigenstates derived from the polyad two-resonance model. This material is available free of charge via the Internet at <http://pubs.acs.org>.

References and Notes

- Moss, R. A.; Jones, M., Jr., Eds. *Carbenes*, Vol. I–II in *Reactive Intermediates in Organic Chemistry Series*, Wiley–Interscience: New York, 1973, Vol. I; 1975, Vol. II.
- Kirmse, W. *Carbene Chemistry*, 2nd ed., Academic: New York, 1971.
- Sciano, J. C. In *Handbook of Organic Photochemistry*; CRC Press: Boca Raton, FL, 1989; Vol. 2; Chapter 9.
- Carey, F. A.; Sundberg, R. J. In *Advanced Organic Chemistry*, Part 3, 3rd ed., Plenum: New York, 1990.
- Weirsum, U. E.; Jenneskens, L. W. In *Gas Phase Reactions in Organic Synthesis*; Vallée, Y., Ed.; Gordon, Breach: Australia, 1997.
- Dean, A. M.; Bozzelli, J. W. In *Gas-Phase Combustion Chemistry*; Gardiner, W. C., Jr. Ed.; Springer: New York, 2000; Chapter 2.
- Bacskay, G. B.; Martoprawiro, M.; Mackie, J. C. *Chem. Phys. Lett.* **1998**, *290*, 391–398.
- Sendt, K.; Ikeda, E.; Bacskay, G. B.; Mackie, J. C. *J. Phys. Chem. A* **1999**, *103*, 1054–1072.
- Martoprawiro, M.; Bacskay, G. B.; Mackie, J. C. *J. Phys. Chem. A* **1999**, *103*, 3923–3934.
- Sendt, K.; Bacskay, G. B.; Mackie, J. C. *J. Phys. Chem. A* **2000**, *104*, 1861–1875.
- Wayne, R. P. In *Chemistry of Atmospheres*, Oxford University Press: Oxford, U.K., 1991; Chapter 8 and references therein.
- Winnewisser, G.; Herbst, E. *Rep. Prog. Phys.* **1993**, *56*, 1209–1273, *Top. Curr. Chem.* **1987**, *139*, 119–172.
- Herbst, E. *Angew. Chem., Int. Ed. Engl.* **1990**, *29*, 595–608.
- Harrison, J. F. *J. Am. Chem. Soc.* **1971**, *93*, 4112–4119.
- Staemmler, V. *Theor. Chim. Acta* **1974**, *35*, 309–327.
- Bauschlicher, C. W., Jr.; Schaefer, H. F., III; Bagus, P. S. *J. Am. Chem. Soc.* **1977**, *99*, 7106–7110.
- Baird, N. C.; Taylor, K. F. *J. Am. Chem. Soc.* **1978**, *100*, 1333–1338.
- Bauschlicher, C. W., Jr. *J. Am. Chem. Soc.* **1980**, *102*, 5492–5493.
- Mueller, P. H.; Rondan, N. G.; Houk, K. N.; Harrison, J. F.; Hooper, D.; Willen, B. H.; Liebman, J. F. *J. Am. Chem. Soc.* **1981**, *103*, 5049–5052.
- Scuseria, G. E.; Durán, M.; MacLagan, R. G. A. R.; Schaefer, H. F., III. *J. Am. Chem. Soc.* **1986**, *108*, 3248–3253.
- Carter, E. A.; Goddard, W. A., III. *J. Phys. Chem.* **1987**, *91*, 4651–4652.
- Carter, E. A.; Goddard, W. A., III. *J. Chem. Phys.* **1988**, *88*, 1752–1763.
- Murray, K. K.; Leopold, D. G.; Miller, T. M.; Lineberger, W. C. *J. Chem. Phys.* **1988**, *89*, 5442–5453.
- Shin, S. K.; Goddard, W. A., III; Beauchamp, J. L. *J. Phys. Chem.* **1990**, *94*, 6963–6969.
- Shin, S. K.; Goddard, W. A., III; Beauchamp, J. L. *J. Chem. Phys.* **1990**, *93*, 4986–4893.
- Weis, B.; Rosmus, P.; Yamashita, K.; Morokuma, K. *J. Chem. Phys.* **1990**, *92*, 6635–6644.
- Gutsev, G. L.; Ziegler, T. *J. Phys. Chem.* **1991**, *95*, 7220–7228.
- Gilles, M. K.; Ervin, K. M.; Ho, J.; Lineberger, W. C. *J. Phys. Chem.* **1992**, *96*, 1130–1141.
- Irikura, K. K.; Goddard, W. A.; Beauchamp, J. L., III. *J. Am. Chem. Soc.* **1992**, *114*, 48–51.
- Russo, N.; Sicilia, E.; Toscano, M. *J. Chem. Phys.* **1992**, *97*, 5031–5036.
- Gobbi, A.; Frenking, G. *J. Chem. Soc., Chem. Commun.* **1993**, *14*, 1162–1164.
- Garcia, V. M.; Castell, O.; Reguero, M.; Callol, R. *Mol. Phys.* **1996**, *87*, 1395–1404.
- Schmidt, T. W.; Bacskay, G. B.; Kable, S. H. *Chem. Phys. Lett.* **1998**, *292*, 80–86.
- Chang, B.-C.; Costen, M. L.; Marr, A. J.; Ritchie, G.; Hall, G. E.; Sears, T. J. *J. Mol. Spectrosc.* **2000**, *202*, 131–143.
- Sendt, K.; Bacskay, G. B. *J. Chem. Phys.* **2000**, *112*, 2227–2238.
- Tsai, T.-C.; Chen, C.-W.; Chang, B.-C. *J. Chem. Phys.* **2001**, *115*, 766–770.
- Chen, C.-W.; Tsai, T.-C.; Chang, B.-C. *J. Mol. Spectrosc.* **2001**, *209*, 254–258.
- Chen, C.-W.; Tsai, T.-C.; Chang, B.-C. *Chem. Phys. Lett.* **2001**, *347*, 73–78.
- Lee, C.-L.; Liu, M.-L.; Chang, B.-C. *J. Chem. Phys.* **2002**, *117*, 3263–3268.
- Lee, C.-L.; Liu, M.-L.; Chang, B.-C. *Phys. Chem. Chem. Phys.* **2003**, *5*, 3859–3863.
- Merer, A. J.; Travis, D. N. *Can. J. Phys.* **1966**, *44*, 1541–1550.
- Hoffmann, R.; Zeiss, G. D.; Van Dine, G. W. *J. Am. Chem. Soc.* **1968**, *90*, 1485–1499.
- Jacox, M. E.; Mulligan, D. E. *J. Chem. Phys.* **1969**, *50*, 3252–3262.
- Patel, R. I.; Stewart, G. W.; Casleton, K.; Gole, J. L.; Lombardi, J. R. *Chem. Phys.* **1980**, *52*, 461–468.
- Kakimoto, M.; Saito, S.; Hirota, E. *J. Mol. Spectrosc.* **1981**, *88*, 300–310.
- Suzuki, T.; Saito, S.; Hirota, E. *J. Mol. Spectrosc.* **1981**, *90*, 447–459.
- Butcher, R. J.; Saito, S.; Hirota, E. *J. Chem. Phys.* **1984**, *80*, 4000–4002.
- Suzuki, T.; Saito, S.; Hirota, E. *Can. J. Phys.* **1984**, *62*, 1328–1335.
- Hakuta, K. *J. Mol. Spectrosc.* **1984**, *106*, 56–63.
- Suzuki, T.; Hirota, E. *J. Chem. Phys.* **1986**, *85*, 5541–5546.
- Schmidt, T. W.; Bacskay, G. B.; Kable, S. H. *J. Chem. Phys.* **1999**, *110*, 11277–11285.
- Schwartz, M.; Marshall, P. *J. Phys. Chem. A* **1999**, *103*, 7900–7906.
- Nauta, K.; Guss, J. S.; Owens, N. L.; Kable, S. H. *J. Chem. Phys.* **2004**, *120*, 3517–3518.
- Liang, J.; Kong, X.; Zhang, X.; Li, H. *J. Mol. Struct. (THEOCHEM)* **2004**, *672*, 133–139.
- Fan, H.; Ionescu, I.; Annesley, C.; Reid, S. A. *Chem. Phys. Lett.* **2003**, *378*, 548–552.
- Fan, H.; Ionescu, I.; Annesley, C.; Cummins, J.; Bowers, M.; Xin, J.; Reid, S. A. *J. Phys. Chem. A* **2004**, *108*, 3732–3738.
- Ionescu, I.; Fan, H.; Annesley, C.; Xin, J.; Reid, S. A. *J. Chem. Phys.* **2004**, *120*, 1164–1167.
- Fan, H.; Ionescu, I.; Xin, J.; Reid, S. A. *J. Chem. Phys.* **2004**, *121*, 8869–8873.
- Ionescu, I.; Fan, H.; Ionescu, E.; Reid, S. A. *J. Chem. Phys.* **2004**, *121*, 8874–8879.
- Fan, H.; Mukarakate, C.; Deselnicu, M.; Tao, C.; Reid, S. A. *J. Chem. Phys.* **2005**, *123*, 014314/1–014314/7.
- Tao, C.; Deselnicu, M.; Fan, H.; Mukarakate, C.; Reid, S. A. *Phys. Chem. Chem. Phys.* **2006**, *8*, 707–713.
- Deselnicu, M.; Mukarakate, C.; Tao, C.; Reid, S. A. *J. Chem. Phys.* **2006**, *124*, 134302/1–224302/11.
- Tao, C.; Mukarakate, C.; Reid, S. A. *J. Chem. Phys.* **2006**, *124*, 224314/1–224314/11.
- Mukarakate, C.; Mishchenko, Y.; Brusse, D.; Tao, C.; Reid, S. A. *Phys. Chem. Chem. Phys.* **2006**, *8*, 4320–4326.
- Tao, C.; Deselnicu, M.; Mukarakate, C.; Reid, S. A. *J. Chem. Phys.* **2006**, *125*, 094305/1–094305/9.
- Tao, C.; Reid, S. A.; Schmidt, T. W.; Kable, S. H. *J. Chem. Phys.* **2007**, *126*, 051105/1–051105/4.

- (67) Herzberg, G. *Molecular Spectra and Molecular Structure II. Infrared and Raman Spectra of Polyatomic Molecules*; Van Nostrand: New York, 1945; pp 205–208.
- (68) Werner, H.-J.; Knowles, P. J.; Lindh, R.; Manby, F. R.; Schütz, M. et al. *MOLPRO*, version 2006.1; a package of ab initio programs; www.molpro.net, 2006.
- (69) Willets, A.; Caw, J. F.; Green, W. H., Jr.; Handy, N. C. *SPECTRO*, version 3.0; a second-order rovibrational perturbation theory program; University Chemical Laboratory: Cambridge, U.K., 1994; extended by J. M. L. martin for generalized second-order resonances.
- (70) Papousek, D.; Aliev, M. R. *Molecular Vibrational-Rotational Spectra, Studies in Physical and Theoretical Chemistry 17*, Elsevier: Amsterdam, 1982; pp 160–163.
- (71) Lehmann, K. K. *Mol. Phys.* **1989**, *66*, 1129–1137.
- (72) Martin, J. M. L.; Taylor, P. R. *Spectrochim. Acta A* **1997**, *53*, 1039–1050.
- (73) Polik, W. F.; van Ommen, J. R.; Ellingson, B. A. *POLYAD*, version 10; a general vibrational resonance fitting and vibrational state prediction program; Hope College: Holland, MI, 2007.
- (74) Wagner, M.; Gamperling, M.; Braun, D.; Phohaska, M.; Hüttner, W. *J. Mol. Struct.* **2000**, *517–518*, 327–334.
- (75) Hedberg, L.; Mills, I. M. *J. Mol. Spectrosc.* **2000**, *203*, 82–95.
- (76) Kuchitsu, K. *J. Chem. Phys.* **1968**, *49*, 4456–4462.
- (77) Kuchitsu, K.; Fukuyama, T.; Morino, Y. *J. Mol. Struct.* **1968**, *1*, 463–479; **1969**, *4*, 41–50.
- (78) Huber, K. P.; Herzberg, G. *Molecular Spectra and Molecular Structure, 4: Constants of Diatomic Molecules*; Van Nostrand Reinhold: New York, 1979.
- (79) Kuchitsu, K.; Morino, Y. *Bull. Chem. Soc. Jpn.* **1965**, *38*, 805–813.
- (80) Tackett, B. S.; Li, Y.; Clouthier, D.; Pacheco, K. L.; Schick, G. A.; Judge, R. H. *J. Chem. Phys.* **2006**, *125*, 114301.